HHS Public Access

Author manuscript

J Tissue Eng Regen Med. Author manuscript; available in PMC 2018 February 01.

Published in final edited form as:

J Tissue Eng Regen Med. 2017 February ; 11(2): 412–424. doi:10.1002/term.1925.

Scaffold-free cartilage subjected to frictional shear stress demonstrates damage by cracking and surface peeling

G. Adam Whitney[1,4], **Karthik Jayaraman**[3], **James E. Dennis**[1,2,4], and **Joseph M. Mansour**[2,3]

[1]Department of Biomedical Engineering, Case Western Reserve University, Cleveland, OH, USA

[2]Department of Orthopaedics, Case Western Reserve University, Cleveland, OH, USA

[3]Department of Mechanical and Aerospace Engineering, Case Western Reserve University, Cleveland, OH, USA

[4]Matrix Biology Program, Benaroya Research Institute, Seattle, WA, USA

Abstract

Scaffold-free engineered cartilage is being explored as a treatment for osteoarthritis. In this study, frictional shear stress was applied to determine the friction and damage behavior of scaffold-free engineered cartilage, and tissue composition was investigated as it relates to damage. Scaffold-free engineered cartilage frictional shear stress was found to exhibit a time-varying response similar to that of native cartilage. However, damage occurred which was not seen in native cartilage, manifesting primarily as tearing through the central plane of the constructs. In engineered cartilage, cells occupied a significantly larger portion of the tissue in the central region where damage was most prominent (18 ± 3% of tissue was comprised of cells in the central region vs. 5 ± 1% in the peripheral region, $p < 0.0001$). In native cartilage, cells comprised between 1% and 4% of tissue for all regions. Average bulk cellularity of engineered cartilage was also greater ($68 \times 10^3 \pm 4 \times 10^3$ vs. $52 \times 10^3 \pm 22 \times 10^3$ cells/mg), though this difference was not significant. Bulk tissue comparisons showed significant differences between engineered and native cartilage in hydroxyproline content (8 ± 2 vs. 45 ± 3 μg HYP/mg dry weight), solid content (12.5 ± 0.4% vs. 17.9 ± 1.2%), shear modulus (0.06 ± 0.02 vs. 0.15 ± 0.07 MPa), and aggregate modulus (0.12 ± 0.03 vs. 0.32 ± 0.14 MPa respectively). These data indicate that enhanced collagen content and more uniform extracellular matrix distribution are necessary to reduce damage susceptibility.

Keywords

Scaffold-free engineered cartilage composition; Frictional shear; Tribology; Mechanical properties; Depth-dependent cellularity; Damage

Corresponding Author: Joseph M. Mansour, Ph.D., 617 Glennan Building, 2123 Martin Luther King Jr. Dr., Case Western Reserve University, Cleveland, OH 44106-7222, Phone: (216) 368-4190, Fax: (216) 368-3007, Mansour@case.edu.

The authors have no professional or financial affiliations to disclose. A brief description of the observed damage resulting from frictional shear stress and cellularity patterns in TE cartilage was previously published in the Case Western Reserve University Department of Orthopaedics journal, Case Orthopaedic Journal, 2011.

1. Introduction

While the median age of patients diagnosed with knee osteoarthritis (OA) in the U.S. is now 55 years of age (Losina *et al.*, 2013), complications associated with revision surgery limit the availability of the gold-standard therapy, total joint replacement (TJR), within the patient demographic younger than 65. No other long-term therapy has been widely accepted for treatment of the younger patient population, leaving a great need for such a viable therapy. We recently demonstrated the generation of large scaffold-free tissue engineered (TE) cartilage sheets in chemically defined medium using chondrocytes from skeletally mature donors (Whitney *et al.*, 2012). We are working toward joint resurfacing using scaffold-free constructs. Scaffold-free constructs present some benefits over scaffold-based methods, such as obviating the challenges of uniform seeding, matching scaffold degradation to extracellular matrix (ECM) production, sterilization, immunogenicity, and breakdown product and crosslinking agent toxicity (Puppi *et al.*, 2010). However, the properties of scaffold-free TE cartilage under multi-axial loading are relatively unexplored.

If TE cartilage is to be used to resurface a joint, it must possess the lubrication and mechanical properties to withstand the multi-axial loads transmitted across articulating joints. Aggregate or Young's modulus are often reported as measures of cartilage mechanical quality, since they are reported to correlate to cartilage strength (Kerin *et al.*, 1998). However, uniaxial properties such as compressive strength may not be predictive of cartilage's ability to function in the multi-axial cyclic loading environment of articulating joints. Tribological evaluation, used to study friction, lubrication, and wear, simultaneously subjects a material to static compression and sliding shear stresses, and may be a better indicator of the functional quality of a tissue than uniaxial mechanical properties. This type of testing is common for engineering materials and devices, such as bearings, and was adapted for characterizing the lubrication of native cartilage as early as 1936 (Jones, 1936). In addition, tribological tests have been used to elucidate the role of lubricin (or PRG4) and other boundary molecules in cartilage lubrication (Jay *et al.*, 1998; Jay *et al.*, 2007; Gleghorn *et al.*, 2007; Gleghorn *et al.*, 2009; Zappone *et al.*, 2008; Schmidt *et al.*, 2007), to characterize the friction response of scaffold TE cartilage (Morita *et al.*, 2006), and to evaluate the damage of native (Jay *et al.*, 2007; Graindorge and Stachowiak, 2000; Lipshitz *et al.*, 1975) and scaffold TE cartilage (Gleghorn *et al.*, 2010) under combined compression and shear.

During preliminary tribological evaluation of our TE constructs, we observed disturbances in the frictional shear force that were not seen when testing native cartilage. We also observed catastrophic damage in the TE constructs, rather than the mild surface wear we were expecting. The nature and extent of the observed damage prompted us to shift our focus to characterizing this damage in hope of reducing these constructs' susceptibility to damage. Damage was predominantly seen in the central region of the constructs. We hypothesized that this pattern of damage would be related to the distribution of the cellular and ECM components. While scaffold-free construct generation obviates the challenges of uniformly seeding cells associated with scaffold-employing techniques, as with scaffold-based constructs, mass transport laws suggest that the cell and ECM distribution will not be uniform at construct maturity (Mahmoudifar and Doran, 2005; Wendt *et al.*, 2005; Sengers

et al., 2005; Vunjak-Novakovic *et al.*, 1999). Specifically, increased access to nutrients and soluble molecules at the construct periphery may promote greater ECM production at the edges, thereby reducing the cell density in that region as compared to the central regions of the construct. The objective of this study was to determine the result of frictional shear stress on damage behavior of scaffold-free TE cartilage. We also characterized tissue composition and static mechanical properties to gain insight into the causes of construct damage resulting from frictional shear stress. To our knowledge, this is the first report of frictional shear stress testing, and cell and ECM distribution, in scaffold-free TE cartilage.

2. Materials and Methods

2.1 Cartilage generation, acquisition, and preparation

Scaffold-free TE cartilage constructs were generated from culture-expanded rabbit chondrocytes, as previously described (Whitney *et al.*, 2012). Briefly, culture expanded articular chondrocytes were seeded at 3×10^6 cells/cm^2 onto polyester membranes with 10 μm diameter pores (PET1009030; Sterlitech, Kent, WA), and then cultured in chondrogenic media for 8 weeks. The construct is suspended in culture medium by the porous membrane, allowing access to culture medium from the upper and lower surface. This results in sheet-like constructs, approximately 4 cm × 4 cm and approximately 400 μm thick, which appear to be more cellular in the central region as opposed to the upper and lower regions. At harvest (8 or 12 weeks), constructs were sectioned into 5 mm diameter punches or 8 mm × 16 mm rectangular samples, then frozen at −20 °C. Prior to mechanical and frictional shear testing, 8 mm ×16 mm samples were trimmed to 5 mm × 14 mm and the excess was used for compositional assays. Healthy bovine cartilage was used as a native cartilage control, since samples comparable in size to TE test samples could not be obtained from rabbit joints. Native bovine samples were taken from the shoulders of steers (approximately 1 year old) collected from abattoirs (Don and Joe's Meats, Seatte, WA; Boris' Kosher Meats, Cleveland, OH) and dissected from the subchondral bone, then frozen at −20 °C until use.

2.2 Frictional shear stress and damage evaluation

Time-varying friction force of scaffold-free TE cartilage and native bovine cartilage was measured on a custom device. Normal load was applied by dead weight, and friction force was measured using a single point load cell that is insensitive to off-axis loads (LCAE-600G; Omega Engineering, Stamford, CT) (Figure 1). Friction force was recorded by a custom LabView (National Instruments, Austin, TX) program at a sampling rate of 40 Hz. The raw friction force signal was rectified and filtered with a finite impulse response lowpass filter, to smooth transients resulting from reciprocation of the counterface. Two device configurations were employed in our experiments: curved and flat. The curved configuration (Figure 1A) was representative of reciprocating the femoral condyle against glass (Caligaris and Ateshian, 2008), and also of the configuration used in some theoretical lubrication models (Ateshian and Wang, 1995; Ateshian, 1997) to represent incongruent joint surfaces such as the knee. In this configuration, unknown contact area precludes calculation of contact stress, so normal loads and frictional shear forces were normalized to the width of the tissue strip (Newtons/millimeter of construct width). The flat configuration (Figure 1B) is similar to that described in the literature (Gleghorn and Bonassar, 2008), and

allows direct calculation of the contact area. Results from testing performed in this configuration are reported as normal and frictional shear stresses, calculated by normalizing the respective forces to contact area. In the curved configuration, 5 mm × 14 mm samples were adhered to hemicylindrical platens with radii of 12.5 mm, so only a portion of the sample length made contact with the counterface. In the flat configuration, 5 mm circular punches were adhered to flat, self-aligning platens, similar to those reported by Gleghorn and Bonassar (Gleghorn and Bonassar, 2008). Two counterface oscillation modes were employed as well, continuous and intermittent. Intermittent mode consisted of oscillation for 10-second intervals followed by compression-only periods, the duration of which increased logarithmically throughout the length of the test. Testing was stopped after 10,000 seconds, or after the coefficient of friction (CoF) had reached equilibrium (a change of less than 0.01 between sequential cycles). CoF was calculated as the measured friction force divided by the normal force. In all experiments, a glass counterface (12-544-1, Fisher Scientific, Pittsburgh, PA) was oscillated against the test specimen. The path length was 56 mm in each direction to provide a high ratio of constant velocity vs. accelerating/decelerating travel in each reciprocation.

To further characterize and investigate possible causes of the damage observed in preliminary studies, the six following experiments were performed. First, we characterized the disturbance in the frictional shear force observed in preliminary studies by comparing the time varying friction response of 3 samples originating from two TE constructs to native cartilage thinned on a cryostat such that the sections included the superficial zone and approximately 400 μm of underlying cartilage (n=3). Native cartilage was thinned to make it more comparable in thickness to TE samples. This test was performed under the same conditions as those used in preliminary studies: PBS lubricant using the curved configuration at a velocity of 25.4 mm/s in intermittent oscillation, with normal loads of 0.44 N/mm of construct width for TE constructs and 0.75 N/mm of construct width for native cartilage.

Second, we wished to increase the power of the previous test in assessing whether the difference in damage behavior between native and TE cartilage observed in preliminary studies was due to the greater thickness of the native cartilage (approximately 3× that of TE). We also asked whether native cartilage from deeper zones, i.e. with the potentially protective superficial zone removed, would exhibit damage in this test setup. In this experiment, test parameters were the same as in the previous experiment, except that the sliding speed was changed to 1 mm/s to assess whether damage was speed-dependent, and continuous oscillation was used. Continuous oscillation was selected for agreement with subsequent experiments, and rationale is given in description of those experiments. For this experiment, 4 additional native cartilage samples were thinned on a vibratome to include the superficial zone, and another 6 samples were taken starting approximately 200 μm below the superficial zone. Three TE samples were taken from 2 additional constructs. Since damage behavior of TE and native cartilage with the superficial zone intact appeared to be the same between this and the previous experiment, those samples were pooled together for damage analysis (n=6 for TE and native cartilage without the articulating surface, and n=7 for native cartilage with the articulating surface).

Third, we wished to determine if differential protease activity between TE cartilage and native cartilage played a role in the damage observed. In this experiment, samples were tested in the flat configuration. A normal load of 0.55 MPa was chosen based on observations from preliminary studies in this configuration in which we observed that TE cartilage exhibited damage at this load. The flat configuration and continuous oscillation were selected to allow friction data from these samples to be used in the next experiment. Test duration was shortened to 4000 seconds since damage appeared to occur early in the first two experiments. The other test parameters, including sliding speed, remained the same as in the previous experiment. Samples from one TE construct were tested in either PBS or in a PBS-based protease inhibitor solution containing 2mM ethylenediaminetetraacetic acid (EDTA), 5 mM benzamidine, 10 mM N-ethymaleimide, and 1 mM phenylmethylsulfonyl fluoride (n=4 in PBS, n=6 in protease inhibitor solution). The maximum frictional shear stress (MFSS) achieved before damage was compared between the PBS and protease inhibitor groups. For native cartilage, 4 samples were tested in each lubricant.

Fourth, to determine if TE constructs failed as a result of exposure to elevated frictional shear stress as would result from poor lubrication, we compared the MFSS achieved by TE cartilage and native cartilage in this test setup (MFSS prior to failure for TE cartilage, and MFSS at equilibrium friction for native cartilage). TE samples from the protease inhibition experiment were pooled together since MFSS was not significantly different between the two lubricant groups, and compared to eight native samples (n=10 for TE, n=8 for native). To gain insight as to whether damage was a result of fatigue or insufficient strength, we also assessed whether damage occurred during the rising portion of the friction curve (suggestive of insufficient strength), or after reaching equilibrium (suggestive of fatigue damage). The number of cycles of shear before TE cartilage damage occurred was also compared to the number of cycles of shear to which native cartilage was subjected. Use of the flat configuration in this experiment allowed direct calculation of normal and frictional shear stresses, and continuous oscillation allowed greater resolution of the time-dependent frictional shear stress as compared to intermittent mode.

Fifth, to determine if the observed pattern of damage was a result of freeze/thaw cycling, the extent of surface peeling of fresh vs. frozen samples was compared. Punches were taken from one additional construct and tested in the flat configuration under 0.55 MPa normal stress, at a sliding speed of 1 mm/s for 4000 seconds. Samples frozen and thawed 3 times (n=7) and fresh samples (n=8) were tested. Surface peeling was quantified on stereomicroscope images in NIH ImageJ (Figure 2).

Sixth, to determine if surface peeling of TE cartilage was caused by the adhesive used to bond cartilage to the platens, in one experiment we used the rough surface of a porous tantalum platen to hold the cartilage in place without the use of an adhesive. Full thickness native and TE cartilage from 3 constructs were tested, n=6 for both. Test parameters were the same as in the previous experiment. Experimental conditions of each of these six experiments are summarized in Table 1.

2.3 Mechanical testing

Prior to frictional shear stress and damage evaluation in the curved configuration, a standard indentation test was performed on some samples. Samples were thawed, equilibrated in the lubricating fluid for that sample, either PBS or protease inhibitor solution, and the thickness was measured using a custom device that detects contact of a micrometer tip with cartilage by monitoring changes in resistance to the flow of a small electrical current. Samples were then adhered by cyanoacrylate to the platen which would be used for frictional shear stress and damage evaluation. A 1.07 millimeter diameter cylindrical porous indenter tip was used. Displacement was measured using a linear variable differential transducer. First, a tare load of 250 mg was applied and displacement was allowed to reach equilibrium; a test load of 1 g was then applied and displacement equilibrated. These loads were chosen to limit sample strain to approximately 20%. Aggregate modulus, and shear modulus were determined as parameters of a biphasic model fit to indentation displacement data as described by Mow and colleagues (Mak *et al.*, 1987; Mow *et al.*, 1989). TE cartilage and native cartilage samples that included the articulating surface were tested. Results from samples taken from the within the same TE construct were averaged, resulting in an n=4 for TE and an n=6 for native cartilage.

2.4 Compositional characterization

Prior to mechanical testing, specimens were trimmed to 5 mm × 14 mm and the excess was collected for biochemical analysis, wet weights obtained, lyophilized, and dry weights measured. The bulk solid content was calculated as a ratio of the solid (dry) to total (wet) weight. Samples were then digested with papain (P4762, Sigma-Aldrich, St. Louis, MO) and the glycosaminoglycan (GAG), DNA, and total collagen, as measured by hydroxyproline (HYP) content were determined for each sample, as previously described (Whitney *et al.*, 2012). GAG and HYP values were normalized to DNA, and to wet and dry weights. Bulk cellularity (cells/mg wet weight) was calculated from the DNA content and wet weight assuming 7.7×10^{-12} grams DNA/chondrocyte (Kim *et al.*, 1988). The rationale for using the thinned rather than full thickness native cartilage for biochemical testing was to have matched mechanical and biochemical data for these samples.

2.5 Histology

After frictional shear stress and damage testing, samples were removed from platens and fixed in 10% formalin, then dehydrated in sequential ethanol baths. They were then embedded in paraffin and sectioned to 5 μm, then stained with safranin O to visualize GAG and counterstained with Fast Green to visualize cell nuclei.

2.6 Histomorphometry for determination of depth-dependent cell and ECM density

Four articular-derived TE constructs were generated and 10 histological micrographs were produced and processed for histomorphometry (Figure 3A). Three full-thickness native cartilage samples were used for comparison. Images were manually segmented in Photoshop (Adobe, San Jose, CA) to indicate the tissue boundary and cells (Figure 3B). Due to the large lacunae that chondrocytes may occupy, it is possible that cells may not appear in the lacunae in histological sections (Hunziker *et al.*, 1992). Void spaces which were

morphologically consistent with lacunae were counted as cells in this analysis. A custom Matlab (Mathworks, Natick, MA) program was used to divide each segmented image into five equal thickness regions throughout the depth of the histological slice (Figure 2C) and calculate the number of cells and area occupied by them within each region. Cell density was defined as cells/mm^2, and a statistic termed "cell area fraction" was defined as the fraction of the area of each region occupied by cells. ECM density was defined as the inverse of cell area fraction and was calculated as [1-cell area fraction × 100].

2.7 Scanning Electron Microscopy (SEM)

Samples were stored at 4 °C in a 0.7% Ruthenium Hexammine Trichloride (RHT) in 1% glutaraldehyde solution in PBS until ready for use. At the time of imaging, samples were fixed in a 1:1 solution of 2% Osmium and 0.7% RHT in PBS for 30 minutes, then dehydrated in graded EtOH baths. They were then dried in a critical point drying device, sputter coated with palladium (Pd), and imaged with a FEI Quanta 3D scanning electron microscope.

2.8 Statistical analysis

Two-sample t-tests with significance set at $p < 0.05$ were used to compare frictional shear stress, mechanical, biochemical, and mass assay results between native and TE cartilage, and to compare surface peeling in the freeze/thaw cycling experiment. The distribution of samples exhibiting greater than 25% surface peeling in the freeze/thaw cycling experiment was also tested for significance at $p < 0.05$ by Fisher's exact test. Linear mixed models, fit using SAS Proc Mixed (version 9.2, SAS, Cary, NC), were used to compare histomorphometry data of native vs. TE cartilage, where random effects were included to account for correlation of multiple samples from the TE cartilage constructs, and of the five regions measured on the same sample. The square root of the variable "cell density" was analyzed in the mixed model to better meet normality assumptions, though summary statistics for this variable are presented on the original scale. Pairwise comparisons of selected means by tissue source (TE vs. native) and region were tested based on model-based estimates, resulting in 5 pairwise comparisons for depth-matched regions between tissue types, and 10 pairwise comparisons by region within each tissue type. To account for multiple testing, significance was set as $p < 0.01$. All summary statistics are presented as means with standard deviations.

3. Results

3.1 Frictional shear stress and damage evaluation

In the initial experiment, assessing friction and damage under intermittent oscillation, friction behavior of scaffold-free TE constructs was similar to that of native cartilage during early time points in this test setup; friction forces were initially low then climbed as the test progressed (Figure 4A). Even when the normal load was different between the two, the CoF in this test setup was remarkably similar for each of them at these early time points (Figure 4B). Divergence from native behavior occurred at later time points, as the friction force was seen to drop (Figure 4A). These samples exhibited cracking in the central region (Figure 4C). Some mild damage was seen on native cartilage, which was qualitatively distinct in

localization, type, and severity (Figure 4D). In the second experiment, in which continuous oscillation was used, TE cartilage exhibited cracking in all 3 samples tested (Figure 5A&B). The minimum damage observed is shown in Figure 5A, while the other 2 appeared more similar to that shown in Figure 5B. Histological cross sections revealed surface peeling on 1 of 4 native cartilage samples that contained the surface zone (Figure 5D). Some samples showed narrowing in the presumable loaded region (Figure 5C), due either to wear or permanent deformation. No cracking was observed. In contrast, native cartilage samples without the superficial zone showed surface peeling in 3 of 6 samples. No damage was observed in 2 of 6 samples (Figure 5E). The remaining sample showed damage somewhat similar to the cracking in the least damaged TE cartilage sample (Figure 5F&A respectively). Since there were no apparent differences in damage with respect to cracking between the first and second studies, samples were pooled together, resulting in 6 of 6 TE cartilage, 0 of 7 native cartilage with the surface zone, and 1 of 6 native cartilage without the surface zone, exhibiting cracking.

In the third study we determined whether protease activity affected the differential damage observed between native and TE cartilage. TE cartilage achieved an MFSS before damage of 0.152 ± 0.039 MPa in PBS, and 0.157 ± 0.039 MPa in protease inhibitor solution. These differences were not statistically significant (n=4 and n=6 respectively). Since native cartilage was undamaged, MFSS corresponded to the peak undulation at equilibrium friction and was, 0.175 ± 0.042 MPa in PBS, and 0.155 ± 0.034 MPa in protease inhibitor solution, which was not statistically significant (n=4 for both lubricants).

Since no statistically significant MFSS differences were seen between lubricant types, samples were pooled for the fourth study comparing the MFSS between native and TE cartilage to determine if damage was the result of exposure to elevated frictional shear stress (n=8 and n=10 respectively). This analysis showed that 10 of 10 TE samples exhibited visually evident surface peeling during the test procedure, while none of the 8 native samples did. Native cartilage MFSS was 0.165 ± 0.037 MPa, while TE cartilage reached an average MFSS of 0.155 ± 0.037 MPa before delaminating. The difference in MFSS for native and TE cartilage was not statistically significant, however TE cartilage delaminated after 11 ± 8 cycles of shear, while native cartilage did not delaminate even after 180 cycles. Nine of 10 TE samples delaminated during the rising portion of the friction response, before reaching equilibrium friction.

The effect of freeze/thaw cycling was determined in the fifth study. No statistically significant differences were observed. By number of samples demonstrating surface peeling, 7 of 8 fresh samples and 6 of 7 freeze/thaw cycled samples exhibited greater than 25% surface peeling. By surface area, fresh sample surface peeling was 77 ± 39% and freeze/thaw cycled samples was 66 ± 43%.

The dependence of surface peeling on the presence of the adhesive used to adhere cartilage to the platens was determined in the sixth and final frictional shear stress study. In the absence of adhesive, surface peeling of TE constructs was 100 ± 0% in TE samples and 0 ± 0% for native cartilage (Supplemental Figure S1).

3.2 Compositional characterization

Biochemical and mass assays indicated that TE tissue was deficient in ECM. Solid content, expressed as a percentage of solid to total weight, was significantly lower in TE as compared to native cartilage (Figure 6D). The apparent reduction of ECM in TE tissue compared to native tissue was further evaluated in terms of the specific cartilage ECM components, GAG and collagen. Average GAG mass normalized to DNA in TE cartilage was less than half that of native tissue. However, one apparent DNA outlier in the native group limited the statistical significance between the TE test group and the native cartilage group (Figure 6A). GAG content was significantly lower when assessed on a wet weight basis (Figure 6A). HYP (a measure for total collagen) was significantly lower in TE vs. native cartilage on both DNA and mass bases (Figure 6B). Bulk cellularity was estimated from DNA content and found to be higher in TE cartilage compared to native cartilage, although with the apparent DNA outlier in the native group, the difference was not statistically significant (Figure 6C).

3.3 Mechanical testing

Results from indentation testing showed TE cartilage to be less stiff than native cartilage. Shear and aggregate moduli for TE cartilage were significantly lower than in native cartilage (by approximately 60%) (Figure 6E).

3.4 Histomorphometry for determination of depth-dependent cell and ECM density

Depth-dependent quantification of cell and ECM density by histomorphometry showed significant differences between TE and native cartilage cell and ECM distributions. Furthermore, the TE cartilage region where failure was most prominent was also the most cellular (Figure 7A-C). Native cartilage cell density was highest at the articulating surface and decreased towards the deeper tissue regions (Figure 7A), while interestingly, cell size showed the opposite trend, although cell size differences within native cartilage were not significant (Figure 7B); as a result, the cell area fraction of native tissue was nearly constant throughout the depth (Figure 7C). TE cartilage cell size followed the same pattern as cell density; both were greatest in the central region (Figure 7A&B), such that this area appeared to contain hypertrophic chondrocytes. Cell size decreased towards the periphery, resulting in two zones that resemble the superficial zone of native cartilage. The combined effect of cell number and cell size resulted in a cell area fraction that was similar to that of native cartilage near the outer surfaces, while in the central regions where cracking was most prominent, cell area fraction was 3 to 4 times higher than in the surface regions, and 9 times higher when comparing the central regions of TE and native cartilage (Figure 7C). Due to the increased cell area fraction, TE cartilage looked more porous and less solid than native cartilage when imaged by SEM (Figure 8).

4. Discussion

Our long-term goal is to repair damaged articular surfaces with living constructs. As part of this goal, we are developing scaffold-free cartilage constructs derived from tissue culture-expanded chondrocytes from skeletally-mature donors. Various groups have reported generation and characterization of scaffold-free TE cartilage (Marlovits *et al.*, 2003; Uenaka *et al.*, 2010; Stoddart *et al.*, 2006; Furukawa *et al.*, 2008; Hoben and Athanasiou, 2008;

Brehm *et al.*, 2006; Grogan *et al.*, 2003; Kitahara *et al.*, 2008; Nagai *et al.*, 2008; Brenner *et al.*, 2013; Khan *et al.*, 2009), however behavior of these constructs under multi-axial, repetitive loading is unknown. In this study, we characterized the behavior of scaffold-free TE cartilage constructs generated by a previously reported method (Whitney *et al.*, 2012) under frictional shear stress. The approach follows that used to characterize friction, lubrication, damage, and wear, of native (Forster and Fisher, 1996; Forster and Fisher, 1999; Graindorge and Stachowiak, 2000; Basalo *et al.*, 2007; Carter *et al.*, 2007; Schmidt *et al.*, 2007; Caligaris *et al.*, 2009; Gleghorn *et al.*, 2010; Lizhang *et al.*, 2011), and scaffold TE cartilage (Chen *et al.*, 2004; Morita *et al.*, 2006; Gleghorn *et al.*, 2007) under combined compression and shear. We also investigated potential explanations for the damage behavior observed during testing.

During frictional shear evaluation, we observed that scaffold-free TE cartilage exhibited a time-varying friction response similar to that of native bovine cartilage, where friction force started at low native-like levels, then increased over time and appeared to approach equilibrium. While published values of friction properties vary widely due to the effects of sliding speed (Gleghorn and Bonassar, 2008), normal load (Gleghorn and Bonassar, 2008; Katta *et al.*, 2009), lubricant and lubrication mode (Gleghorn and Bonassar, 2008), contact area (Carter *et al.*, 2007), and counterface (Patel and Spector, 1997), the mean equilibrium CoF (average friction force of last shear cycle divided by normal force) measured here for native cartilage (0.387 ± 0.087), is within the range of values reported by others (Ikeuchi *et al.*, 1994; Forster and Fisher, 1996). The behavior of TE cartilage deviated from that of native cartilage in our test setup, in that TE cartilage exhibited internal cracking and surface peeling, while the interior of native cartilage was undamaged in all but one sample (a crack near the surface), although some wear was seen on the surface. We wished to identify the cause of this damage, as a step towards reducing the susceptibility of these constructs to damage.

Various compositional, structural, and specimen processing variables could have influenced the mechanical properties of these constructs, thus governing or affecting the observed damage. These variables include, but are not limited to: construct thickness, protease activity, poor lubrication resulting in exposure to excessive frictional shear stresses, pre-existing damage due to freeze/thaw cycling, construct-adhesive interactions, and construct weakness in the central region due to limited ECM or poor ECM quality. In this investigation, we assessed tissue thickness, protease activity, elevated frictional shear stress, freeze/thaw cycling, presence of adhesive, depth-dependent ECM quantity, and bulk ECM quality. In the experiments and assays utilized here, we did not detect any significant role of protease activity, freeze/thaw cycling, or presence of adhesive. While we did not investigate lubrication modes, damage of TE cartilage occurred at an average frictional shear stress below that to which native cartilage was exposed without incurring damage (0.155 ± 0.037 MPa vs. 0.165+/-0.037 MPa respectively) although the difference was not statistically significant. This indicates that poor lubrication (increased exposure to frictional shear stress as compared to native cartilage) is not the cause of the observed damage, and thus the lack of lubricin, nor the lack of other protective lubrication mechanisms, are not the cause of the observed damage behavior. The lack of significance between the MFSS of TE cartilage and native cartilage is surprising given that TE cartilage showed surface peeling. The variability

in MFSS measurements is no doubt a factor limiting significance. Yet, this does not change the conclusion that TE cartilage was not failing due to exposure to elevated frictional shear stress. Tissue thickness, however, may influence damage susceptibility, since some thinned native cartilage did exhibit damage. However, even in thinned native cartilage showing damage, only one specimen showed damage similar to that of TE cartilage (Figure 5A&F). Also, specimens from two different depths within native cartilage that are known to have variable composition were tested. Since a higher proportion of samples that do not include the superficial zone exhibited various types of damage, as compared to those including the superficial zone, it is suggested that composition or structure dominate thickness as the variable of interest. In agreement with that suggestion, is the disparate composition between native and TE cartilage. TE cartilage, which consistently exhibited cracking and surface peeling, contained only 70% as much solid content (ECM) as compared to thinned native cartilage that included the superficial zone (12.5 ± 0.4% vs. 17.9 ± 1.2% respectively). On a wet weight basis, the TE cartilage ECM only contained 63% as much GAG, and 13% as much HYP, as did the native cartilage ECM.

GAG and collagen were quantified in this study because they are known to be largely responsible for the mechanical properties of cartilage; collagen supports tensile loads (Schmidt *et al.*, 1990), while GAG indirectly supports compressive loads through recruiting interstitial fluid (Kempson *et al.*, 1970; Krishnan *et al.*, 2004). Not surprisingly, GAG comprises 21% of dry weight of human femoral condyle cartilage (Anderson *et al.*, 1964), and collagen comprises 67% of the dry weight of human medial femoral condyle cartilage (Lipshitz *et al.*, 1975). Given the lack of ECM, especially collagen and GAG, it is not surprising that stiffness, measured as both shear and aggregate modulus were also low; roughly one-third that of thinned native cartilage. While low compared to native, the aggregate modulus of these scaffold-free TE constructs was similar to that previously reported by our colleagues (Gilpin *et al.*, 2010) and stiffer than some scaffold-based constructs described by others (Chung *et al.*, 2008).

In light of the low solid, GAG, and collagen, content of the ECM, and the resulting low mechanical properties, it is not surprising that TE constructs failed at loads where native cartilage did not (study 3 and study 5, Supplemental Figure S1). The pattern of damage, cracking in the central region, which sometimes resulted in construct splitting by surface peeling, suggested the greatest deficit in ECM was found in the central region. Depth-dependent histomorphometry confirmed that the central region was more cellular than the outer regions, resulting in only 86 ± 3% of the ECM compared to the surface which was articulated against the glass counterface.

The lack of ECM in this region is reflected by the increased amount of tissue occupied by cells. One of the benefits of the scaffold-free approach to cartilage engineering is the uniform distribution of cells at construct initiation, since uniform cell seeding in scaffolds can be difficult to achieve (Thevenot *et al.*, 2008). However, it was not previously known if scaffold-free construct cell distribution remained uniform throughout maturity. We found that the two-sided-diffusion construct generation method employed here, resulted in heterogeneous cell distribution after culture (approximately 250% more cells in the central then the peripheral regions, Figure 7A). Furthermore, cells were also largest in the central

region (Figure 7B). The combined effect of increased cell number and increased cell size compounded to result in a cell area fraction in the central region of more than three times that of the peripheral regions (Figure 7C), resulting in the approximately 14% decrease in ECM quantity by area.

The cell distribution was distinctly different in native tissue, which showed slightly decreasing cell density (Figure 7A), and that cell size tended to increase (Figure 7B) throughout the depth of the tissue. These findings in native tissue are in agreement with published literature (Jadin *et al.*, 2005). Interestingly, these inverse trends combined to result in a nearly uniform cell area fraction through the depth of the tissue (Figure 7C). Also of interest, the cell area fraction at the periphery of the TE constructs was similar to the cell area fraction at the articulating surface of native cartilage (Figure 5C).

This distribution of cellular and ECM components is likely influenced by mass transport, which has been implicated in cell and ECM distribution in many tissue engineering paradigms (Wendt *et al.*, 2005). Presumably, cells in the periphery of the construct have the greatest access to nutrients and other differentiation factors in the culture medium, while the central region has limited access due to depletion by the outer regions and the slow rates of diffusion. The similar cell area fraction of TE cartilage at the periphery to the native cartilage superficial zone (Figure 7C), suggests that increased access to culture medium may produce a construct similar to native cartilage in this regard. While it is not known how the proportion of GAG and collagen change throughout the depth of the construct, increasing the overall proportion of ECM is likely to increase gross GAG and collagen content, and improve mechanical properties. Improved delivery of nutrients and differentiation factors may be possible through convective transport such as perfusion (Wendt *et al.*, 2005; Pazzano *et al.*, 2000; Berson *et al.*, 2002; Davisson *et al.*, 2002).

Limitations of this study include the use of native cartilage control from a different species and anatomical location as compared to chondrocytes used to generate TE constructs, mechanical and biochemical characterization of partial-thickness native cartilage, use of unknown lubrication regimes for frictional shear stress testing, differences between our test setup and native articulating joint function, and lack of depth-dependent ECM content characterization. The rationale for using bovine cartilage is given in the methods section. In a similar study on native bovine knee cartilage, Lizhang *et al.* found that native bovine knee cartilage exhibited damage only at compressive stresses and testing durations in large excesses of those we employed here (Lizhang *et al.*, 2011). Their results suggest that native bovine knee cartilage would have shown the same results, with respect to damage, as hip cartilage, in this study. While using partial-thickness native cartilage presents some limitations in comparing TE to native cartilage, in this study it allows sample-matched comparison of mechanical and biochemical properties. Since biochemical and mechanical comparisons were made against native samples containing superficial and medial zone regions, and GAG concentration in full-thickness native cartilage has been reported to increase as a function of depth (Franzén *et al.*, 1981), the disparity in GAG content between TE constructs and native cartilage may be greater if compared to full thickness native cartilage; collagen distribution has been reported to be uniform in full thickness cartilage (Lipshitz *et al.*, 1975). However, the biochemical property results presented here are

comparable to data we previously reported on comparisons to full thickness native rabbit cartilage, showing collagen to be more deficient than GAG in constructs generated using these methods (Whitney *et al.*, 2012). The disparity of aggregate modulus compared to full thickness cartilage would also likely increase, since compressive stiffness is known to be depth-dependent (Schinagl *et al.*, 1996). Lubrication regime characterization was precluded in these studies by construct damage, since such characterization involves equilibrium CoF measurements across a wide range of normal loads (Gleghorn and Bonassar, 2008). Construct damage usually occurred prior to reaching equilibrium CoF, and damage changed the time varying friction pattern (Figure 4B). Limitations on determining whether the constructs are suitable for *in vivo* testing are introduced by the test setup, which does not replicate *in vivo* conditions. It has been shown that the CoF (and thus frictional shear stress) can be maintained near initial friction values under physiological conditions, including when the cartilage contact area migrates as described by Caligaris and Ateshian (Caligaris and Ateshian, 2008). However, comparison to native cartilage under the same conditions showed a clear difference in the ability of these constructs to bear frictional shear stresses. The limitation of not measuring depth-dependent ECM composition is that conclusive determination of whether the cause of damage in the central region was lack of ECM quantity or quality can not be made. However, lower percentage of ECM in the central region indicates that even if the quality were the same as the outer regions, this region would remain the weakest portion.

In conclusion, bulk compositional, mechanical, and frictional shear stress characterization of these scaffold-free constructs all point towards construct weakness rather than elevated frictional shear stress as the cause of damage. Furthermore, despite uniform cell seeding methods, depth-dependent cell and ECM distribution were not uniform after tissue culture. While the damage location was not quantified, and thus correlation of damage location to cellular and ECM distributions can not be formally measured, the final ECM and cellular distributions are consistent with the predominant damage observed. That this damage occurred under relatively low normal and frictional shear stresses indicates improvements are needed before these constructs are applied to joint surfaces. Improvements in cell and ECM distribution, and ECM content, may be possible by enhancing the mass transfer of culture medium and cellular waste products.

Supplementary Material

Refer to Web version on PubMed Central for supplementary material.

Acknowledgements

The authors thank Amad Awadallah for histologic processing, Hisashi Mera, Thomas Kean, and Nell Ginley for biochemical assay development, Mark Weidenbecher and Amad Awadallah for assistance with tissue culture methodology, and Mark Scluchter for statistical analysis assistance. Research reported in this publication was supported by the National Institute of Arthritis and Musculoskeletal and Skin Diseases (NIAMS), part of the National Institutes of Health, under Award Number P01 AR053622 (J.E.D. & J.M.M), the National Institute of Dental and Craniofacial Research, Award Number R01 DE015322 (J.E.D.), and the Ruth L. Kirschstein National Research Service Award T32 AR007505 from the NIH NIAMS. The content is solely the responsibility of the authors and does not necessarily represent the official views of the National Institutes of Health.

References

Anderson CE, Ludowieg J, Harper HA, et al. The composition of the organic component of human articular cartilage: relationship to age and degenerative joint disease. J Bone Joint Surg Am. 1964; 46(6):1176. [PubMed: 14214351]

Ateshian GA, Wang H. A theoretical solution for the frictionless rolling contact of cylindrical biphasic articular cartilage layers. J Biomech. 1995; 28(11):1341–1355. [PubMed: 8522547]

Ateshian GA. A theoretical formulation for boundary friction in articular cartilage. J Biomech Eng. 1997; 119(1):81–86. [PubMed: 9083853]

Basalo IM, Chahine NO, Kaplun M, et al. Chondroitin sulfate reduces the friction coefficient of articular cartilage. J Biomech. 2007; 40(8):1847–1854. [PubMed: 17084404]

Berson RE, Pieczynski WJ, Svihla CK, et al. Enhanced mixing and mass transfer in a recirculation loop results in high cell densities in a roller bottle reactor. Biotechnol Prog. 2002; 18(1):72–77. [PubMed: 11822902]

Brehm W, Aklin B, Yamashita T, et al. Repair of superficial osteochondral defects with an autologous scaffold-free cartilage construct in a caprine model: implantation method and short-term results. Osteoarthr Cartil. 2006; 14(12):1214–1226. [PubMed: 16820305]

Brenner JM, Kunz M, Tse MY, et al. Development of large engineered cartilage constructs from a small population of cells. Biotechnol Prog. 2013; 29(1):213–221. [PubMed: 23197468]

Caligaris M, Ateshian GA. Effects of sustained interstitial fluid pressurization under migrating contact area, and boundary lubrication by synovial fluid, on cartilage friction. Osteoarthr Cartil. 2008; 16(10):1220–1227. [PubMed: 18395475]

Caligaris M, Canal CE, Ahmad CS, et al. Investigation of the frictional response of osteoarthritic human tibiofemoral joints and the potential beneficial tribological effect of healthy synovial fluid. Osteoarthr Cartil. 2009; 17(10):1327–1332. [PubMed: 19410031]

Carter MJ, Basalo IM, Ateshian GA. The temporal response of the friction coefficient of articular cartilage depends on the contact area. J Biomech. 2007; 40(14):3257–3260. [PubMed: 17490673]

Chen AC, Klisch SM, Bae WC, et al. Mechanical characterization of native and tissue-engineered cartilage. Methods Mol Med. 2004; 101(9):157–190. [PubMed: 15299215]

Chung C, Erickson IE, Mauck RL, et al. Differential behavior of auricular and articular chondrocytes in hyaluronic acid hydrogels. Tissue Eng Part A. 2008; 14(7):1121–1131. [PubMed: 18407752]

Davisson T, Sah RL, Ratcliffe A. Perfusion increases cell content and matrix synthesis in chondrocyte three-dimensional cultures. Tissue Eng. 2002; 8(5):807–816. [PubMed: 12459059]

Forster H, Fisher J. The influence of continuous sliding and subsequent surface wear on the friction of articular cartilage. Proc Inst Mech Eng H. 1999; 213(4):329–345. [PubMed: 10466364]

Forster H, Fisher J. The influence of loading time and lubricant on the friction of articular cartilage. Proc Inst Mech Eng H. 1996; 210(2):109–119. [PubMed: 8688115]

Franzén A, Inerot S, Hejderup SO, et al. Variations in the composition of bovine hip articular cartilage with distance from the articular surface. Biochem J. 1981; 195(3):535–543. [PubMed: 7316972]

Furukawa KS, Imura K, Tateishi T, et al. Scaffold-free cartilage by rotational culture for tissue engineering. J Biotechnol. 2008; 133(1):134–145. [PubMed: 17913274]

Gilpin DA, Weidenbecher MS, Dennis JE. Scaffold-free tissue-engineered cartilage implants for laryngotracheal reconstruction. Laryngoscope. 2010; 120(3):612–617. [PubMed: 20058322]

Gleghorn JP, Bonassar LJ. Lubrication mode analysis of articular cartilage using Stribeck surfaces. J Biomech. 2008; 41(9):1910–1918. [PubMed: 18502429]

Gleghorn JP, Doty SB, Warren RF, et al. Analysis of frictional behavior and changes in morphology resulting from cartilage articulation with porous polyurethane foams. J Orthop Res. 2010; 28(10): 1292–1299. [PubMed: 20309861]

Gleghorn JP, Jones ARC, Flannery CR, et al. Boundary mode frictional properties of engineered cartilaginous tissues. Eur Cell Mater. 2007; 14:20–29. [PubMed: 17676563]

Gleghorn JP, Jones ARC, Flannery CR, et al. Boundary mode lubrication of articular cartilage by recombinant human lubricin. J Orthop Res. 2009; 27(6):771–777. [PubMed: 19058183]

Graindorge S, Stachowiak G. Changes occurring in the surface morphology of articular cartilage during wear. Wear. 2000; 241(2):143–150.

Grogan SP, Rieser F, Winkelmann V, et al. A static, closed and scaffold-free bioreactor system that permits chondrogenesis in vitro. Osteoarthr Cartil. 2003; 11(6):403–411. [PubMed: 12801480]

Henderson JH, Welter JF, Mansour JM, et al. Cartilage tissue engineering for laryngotracheal reconstruction: Comparison of chondrocytes from three anatomic locations in the rabbit. Tissue Eng. 2007; 13(4):843–853. [PubMed: 17394383]

Hoben GM, Athanasiou KA. Creating a spectrum of fibrocartilages through different cell sources and biochemical stimuli. Biotechnol Bioeng. 2008; 100(3):587–598. [PubMed: 18078296]

Hunziker EB, Ludi A, Herrmann W. Preservation of cartilage matrix proteoglycans using cationic dyes chemically related to ruthenium hexaammine trichloride. J Histochem Cytochem. 1992; 40(7): 909–917. [PubMed: 1376743]

Ikeuchi, K., Oka, M., Kubo, S. The relation between friction and creep deformation in articular cartilage. In: Dawson, D.Taylor, CM.Childs, THC., et al., editors. Tribology Series. Elsevier; 1994. p. 247-252.

Jadin KD, Wong BL, Bae WC, et al. Depth-varying density and organization of chondrocytes in immature and mature bovine articular cartilage assessed by 3d imaging and analysis. J Histochem Cytochem. 2005; 53(9):1109–1119. [PubMed: 15879579]

Jay GD, Haberstroh K, Cha CJ. Comparison of the boundary-lubricating ability of bovine synovial fluid, lubricin, and Healon. J Biomed Mater Res. 1998; 40(3):414–418. [PubMed: 9570073]

Jay GD, Torres JR, Rhee DK, et al. Association between friction and wear in diarthrodial joints lacking lubricin. Arthritis Rheum. 2007; 56(11):3662–3669. [PubMed: 17968947]

Jones ES. Joint lubrication. The Lancet. 1936; 227(5879):1043–1045.

Katta J, Jin Z, Ingham E, et al. Effect of nominal stress on the long term friction, deformation and wear of native and glycosaminoglycan deficient articular cartilage. Osteoarthr Cartil. 2009; 17(5):662–668. [PubMed: 19028431]

Kempson GE, Muir H, Swanson SA, et al. Correlations between stiffness and the chemical constituents of cartilage on the human femoral head. Biochim Biophys Acta. 1970; 215(1):70–77. [PubMed: 4250263]

Kerin AJ, Wisnom MR, Adams MA. The compressive strength of articular cartilage. Proc Inst Mech Eng H. 1998; 212(4):273–280. [PubMed: 9769695]

Khan AA, Suits JMT, Kandel RA, et al. The effect of continuous culture on the growth and structure of tissue-engineered cartilage. Biotechnol Prog. 2009; 25(2):508–515. [PubMed: 19294749]

Kim Y, Sah R, Doong J. Fluorometric assay of DNA in cartilage explants using Hoechst 33258. Anal Biochem. 1988; 174:168–176. [PubMed: 2464289]

Kitahara S, Nakagawa K, Sah RL, et al. In vivo maturation of scaffold-free engineered articular cartilage on hydroxyapatite. Tissue Eng Part A. 2008; 14(11):1905–1913. [PubMed: 18620479]

Krishnan R, Kopacz M, Ateshian GA. Experimental verification of the role of interstitial fluid pressurization in cartilage lubrication. J Orthop Res. 2004; 22(3):565–570. [PubMed: 15099636]

Lipshitz H, Etheredge R, Glimcher MJ. In vitro wear of articular cartilage. J Bone Joint Surg Am. 1975; 57(4):527–534. [PubMed: 1141265]

Lizhang J, Fisher J, Jin Z, et al. The effect of contact stress on cartilage friction, deformation and wear. Proc Inst Mech Eng H. 2011; 225(5):461–475. [PubMed: 21755776]

Losina E, Weinstein AM, Reichmann WM, et al. Lifetime risk and age of diagnosis of symptomatic knee osteoarthritis in the US. Arthritis Care Res. 2013; 65(5):703–711.

Mahmoudifar N, Doran PM. Tissue engineering of human cartilage and osteochondral composites using recirculation bioreactors. Biomaterials. 2005; 26(34):7012–7024. [PubMed: 16039710]

Mak AF, Lai WM, Mow VC. Biphasic indentation of articular cartilage—I. Theoretical analysis. J Biomech. 1987; 20(7):703–714. [PubMed: 3654668]

Marlovits S, Tichy B, Truppe M, et al. Chondrogenesis of aged human articular cartilage in a scaffold-free bioreactor. Tissue Eng. 2003; 9(6):1215–1226. [PubMed: 14670109]

Morita Y, Tomita N, Aoki H, et al. Frictional properties of regenerated cartilage in vitro. J Biomech. 2006; 39(1):103–109. [PubMed: 16271593]

Mow VC, Gibbs MC, Lai WM, et al. Biphasic indentation of articular cartilage—II. A numerical algorithm and an experimental study. J Biomech. 1989; 22(8-9):853–861. [PubMed: 2613721]

Nagai TT, Sato MM, Furukawa KSK, et al. Optimization of allograft implantation using scaffold-free chondrocyte plates. Tissue Eng Part A. 2008; 14(7):1225–1235. [PubMed: 18489244]

Patel AM, Spector M. Tribological evaluation of oxidized zirconium using an articular cartilage counterface: a novel material for potential use in hemiarthroplasty. Biomaterials. 1997; 18(5):441–447. [PubMed: 9061186]

Pazzano D, Mercier KA, Moran JM, et al. Comparison of chondrogensis in static and perfused bioreactor culture. Biotechnol Prog. 2000; 16(5):893–896. [PubMed: 11027186]

Puppi D, Chiellini F, Piras AM, et al. Polymeric materials for bone and cartilage repair. Progress in Polymer Science. 2010; 35(4):403–440.

Schinagl RM, Ting MK, Price JH, et al. Video microscopy to quantitate the inhomogeneous equilibrium strain within articular cartilage during confined compression. Ann Biomed Eng. 1996; 24(4):500–512. [PubMed: 8841725]

Schmidt MB, Mow VC, Chun LE, et al. Effects of proteoglycan extraction on the tensile behavior of articular cartilage. J Orthop Res. 1990; 8(3):353–363. [PubMed: 2324854]

Schmidt TA, Gastelum NS, Nguyen QT, et al. Boundary lubrication of articular cartilage: Role of synovial fluid constituents. Arthritis Rheum. 2007; 56(3):882–891. [PubMed: 17328061]

Sengers BG, Heywood HK, Lee DA, et al. Nutrient utilization by bovine articular chondrocytes: a combined experimental and theoretical approach. J Biomech Eng. 2005; 127(5):758–766. [PubMed: 16248305]

Stoddart MJ, Ettinger L, Häuselmann HJ. Enhanced matrix synthesis in de novo, scaffold free cartilage-like tissue subjected to compression and shear. Biotechnol Bioeng. 2006; 95(6):1043–1051. [PubMed: 16804949]

Thevenot P, Nair A, Dey J, et al. Method to analyze three-dimensional cell distribution and infiltration in degradable scaffolds. Tissue Eng Part C: Methods. 2008; 14(4):319–331. [PubMed: 19055358]

Uenaka K, Imai S, Ando K, et al. Relation of low-intensity pulsed ultrasound to the cell density of scaffold-free cartilage in a high-density static semi-open culture system. J Orthop Sci. 2010; 15(6): 816–824. [PubMed: 21116901]

Vunjak-Novakovic G, Martin I, Obradovic B, et al. Bioreactor cultivation conditions modulate the composition and mechanical properties of tissue-engineered cartilage. J Orthop Res. 1999; 17(1): 130–138. [PubMed: 10073657]

Wendt D, Jakob M, Martin I. Bioreactor-based engineering of osteochondral grafts: from model systems to tissue manufacturing. J Biosci Bioeng. 2005; 100(5):489–494. [PubMed: 16384786]

Whitney GA, Mera H, Weidenbecher M, et al. Methods for producing scaffold-free engineered cartilage sheets from auricular and articular chondrocyte cell sources and attachment to porous tantalum. Biores Open Access. 2012; 1(4):157–165. [PubMed: 23514898]

Zappone B, Greene GW, Oroudjev E, et al. Molecular aspects of boundary lubrication by human lubricin: effect of disulfide bonds and enzymatic digestion. Langmuir. 2008; 24(4):1495–1508. [PubMed: 18067335]

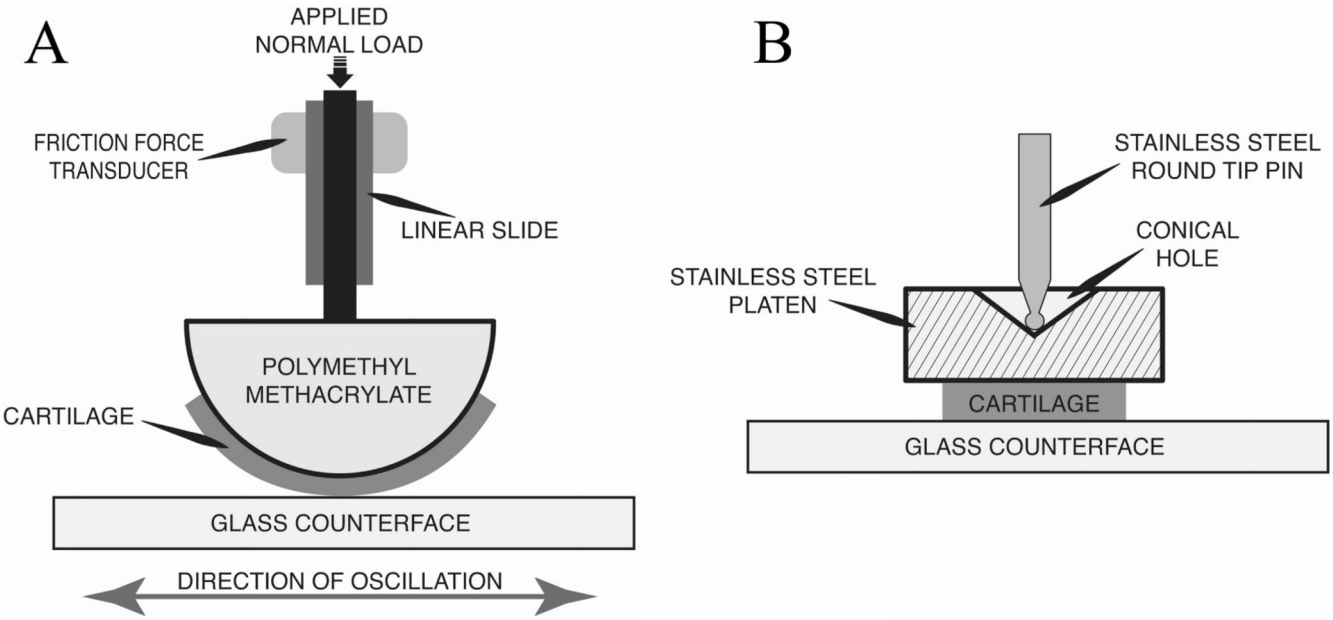

Figure 1. Tribological testing device configuration

A) Load application and measurement schematic with hemicylindrical mount. B) The flat mount utilizing a self-aligning platen. The hemicylindrical and flat mounts were interchangeable in the device.

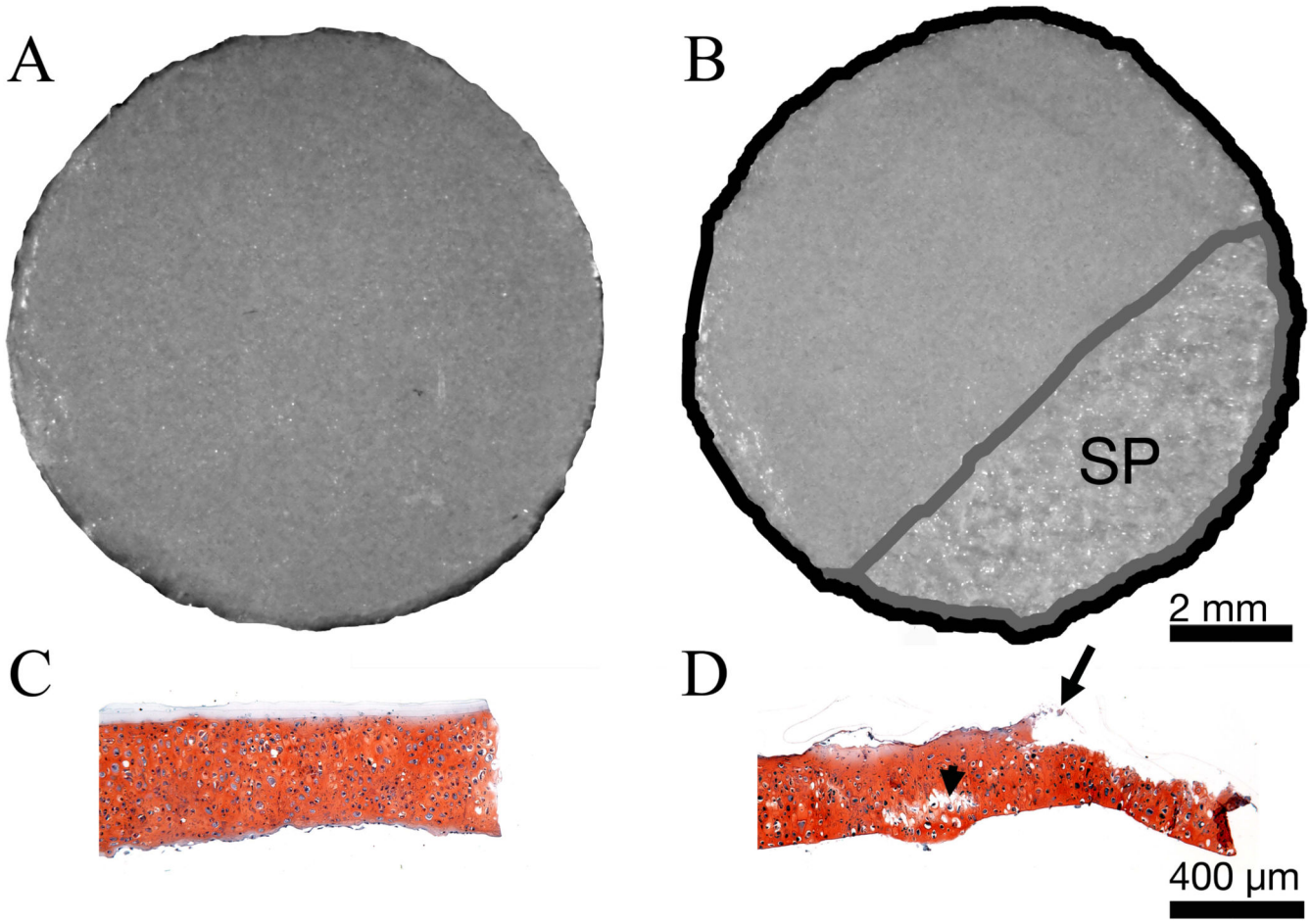

Figure 2. Quantification of surface peeling (SP) in flat configuration

Representative stereomicroscope (A&B) and safranin O stained histological cross section (C&D) images of TE cartilage taken before (A&C), and after (B&D) exposure to frictional shear stress. Area exhibiting SP appeared mottled in stereomicroscope images (B). Damage was determined as the ratio of the area of SP (B, outlined in gray) to the total surface area (B, outlined in black). SP was also evident in histological cross sections (D, starting at the arrow and continuing the length of the section to the right). Internal cracking (arrowhead) is also seen in D. Scale bars in B and D also apply to A and C respectively.

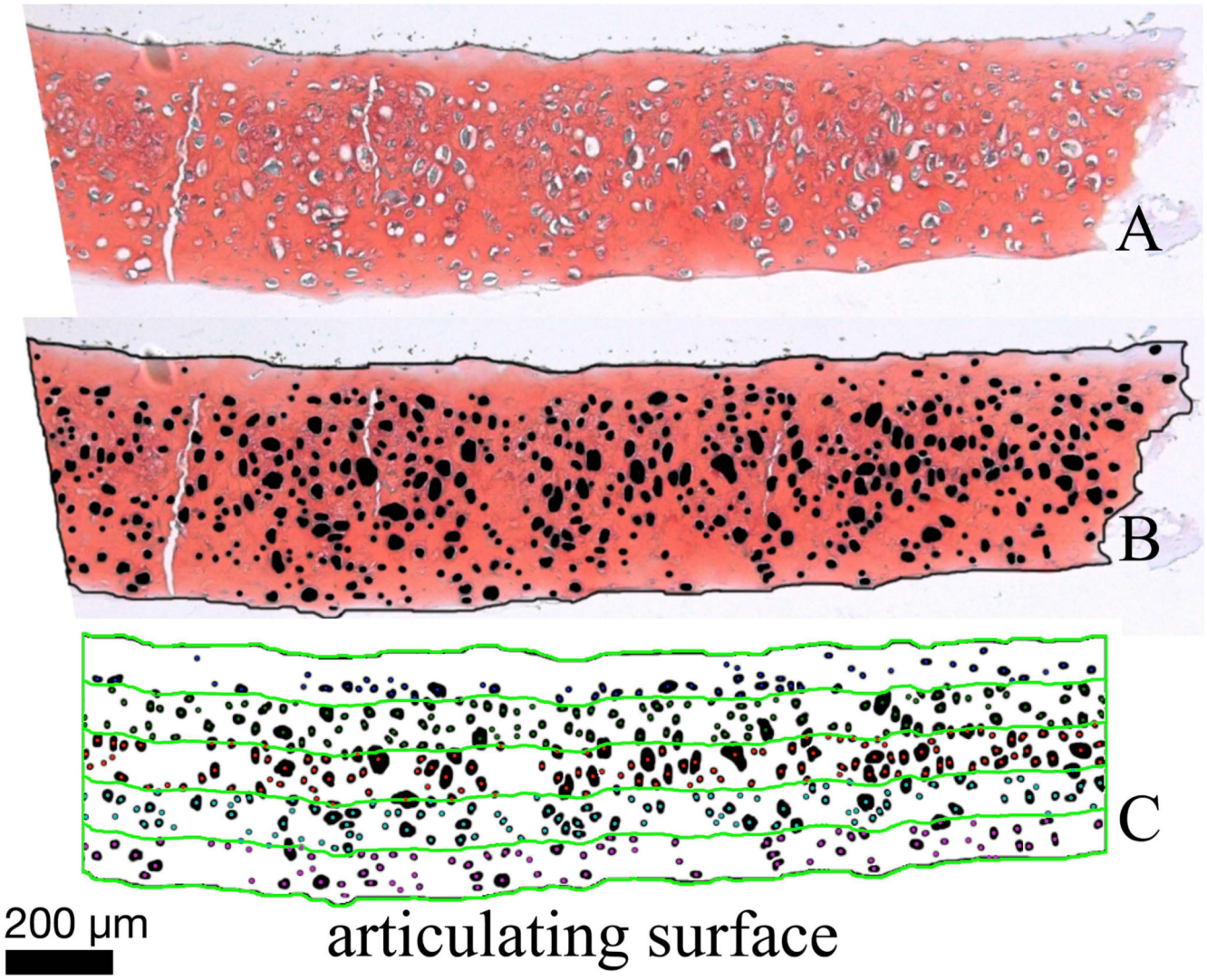

Figure 3. Histomorphometry methods

Safranin O stained histological cross sections (A) were manually segmented in Photoshop to create a mask indicating the location of the tissue boundary (black border around tissue) and the lacunae (black circles) within the tissue (B). Masks were then analyzed with a custom Matlab program to divide the tissue into five equal regions (C) and calculate the number of cells and the area occupied by cells within each region.

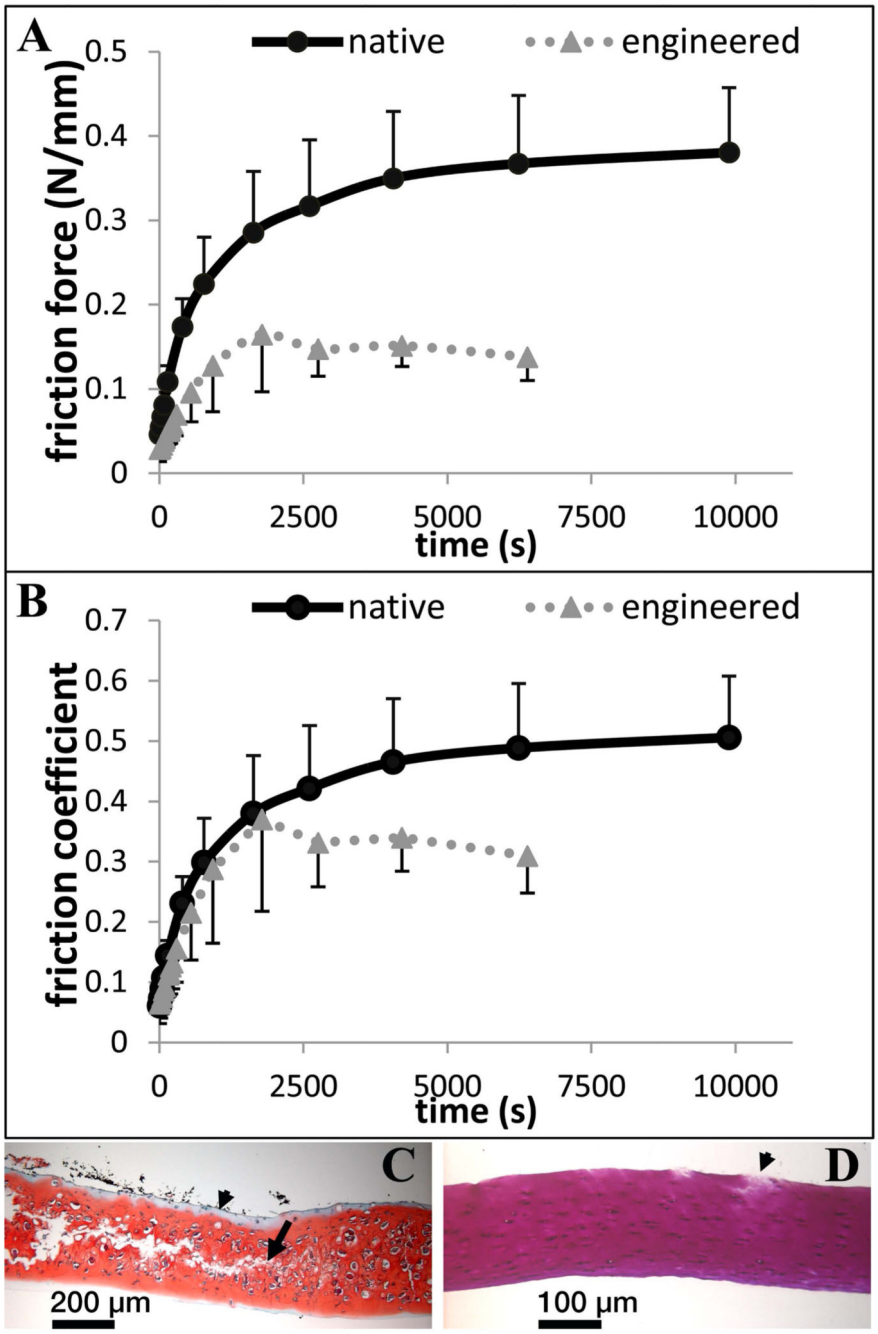

Figure 4. Friction measurements in curved test setup

Friction force (A) and coefficient of friction (B) data for TE and native cartilage. C) Representative safranin O stained histological cross section of TE cartilage. Internal cracking (starting at the arrow and continuing left) is evident. Adhesive can be seen as the unstained region on the upper surface of the tissue (arrowhead). India ink was used to mark the adhered side of the tissue, and can be seen as black fragments near the upper surface. D) Representative toluene blue stained histological cross section of native cartilage. Minimal damage to the upper (adhered) surface of the specimen is shown (arrow).

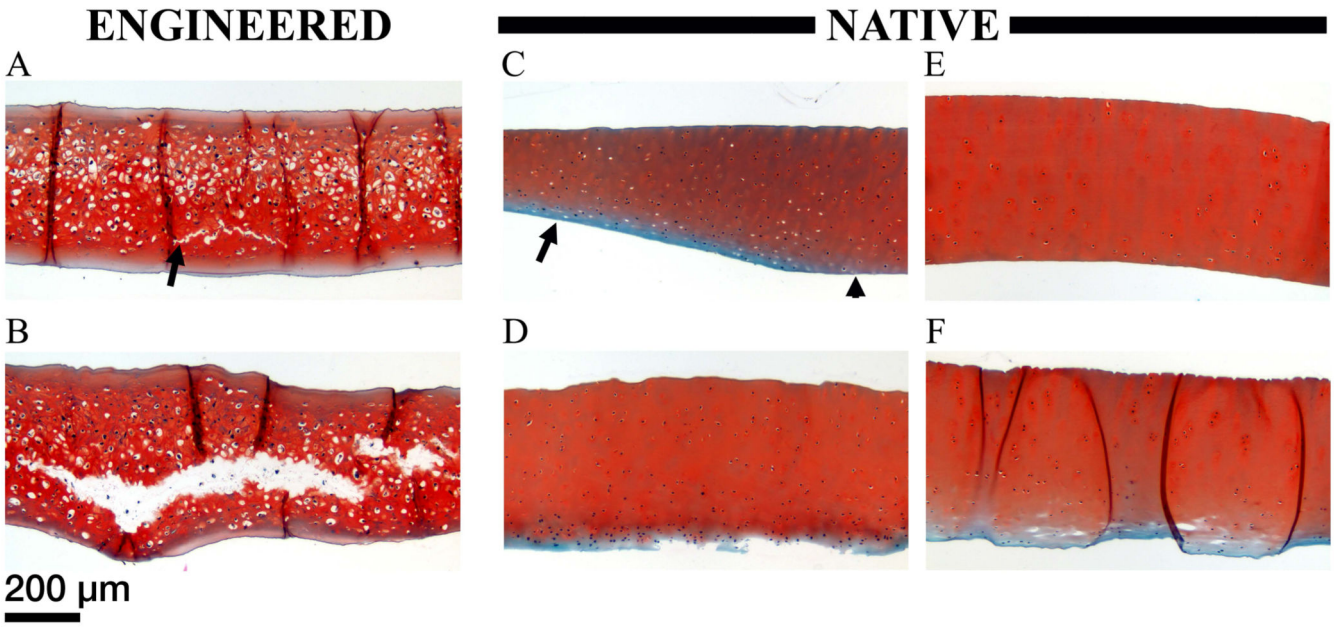

Figure 5. Damage characterization of TE and thinned native cartilage in the curved setup

Safranin O stained histological cross sections of TE cartilage (A&B), native cartilage including the superficial zone (C&D), and native cartilage without the superficial zone (E&F), after exposure to frictional shear stress. The range of damage in each sample group is shown. A) Minimal cracking (arrow) observed in TE cartilage. B) Extensive cracking observed in TE cartilage. C) Narrowing of native cartilage including the superficial zone in the presumed loaded region (arrow), as opposed to the presumed unloaded region (arrowhead). D) Wear of native cartilage including the superficial zone. E) No apparent damage to native cartilage without the superficial zone. F) Minimal cracking (white space within the tissue) observed in native cartilage without the superficial zone. The dark lines running vertically through this sample section are sectioning artifacts (folds). All images are presented at the same scale.

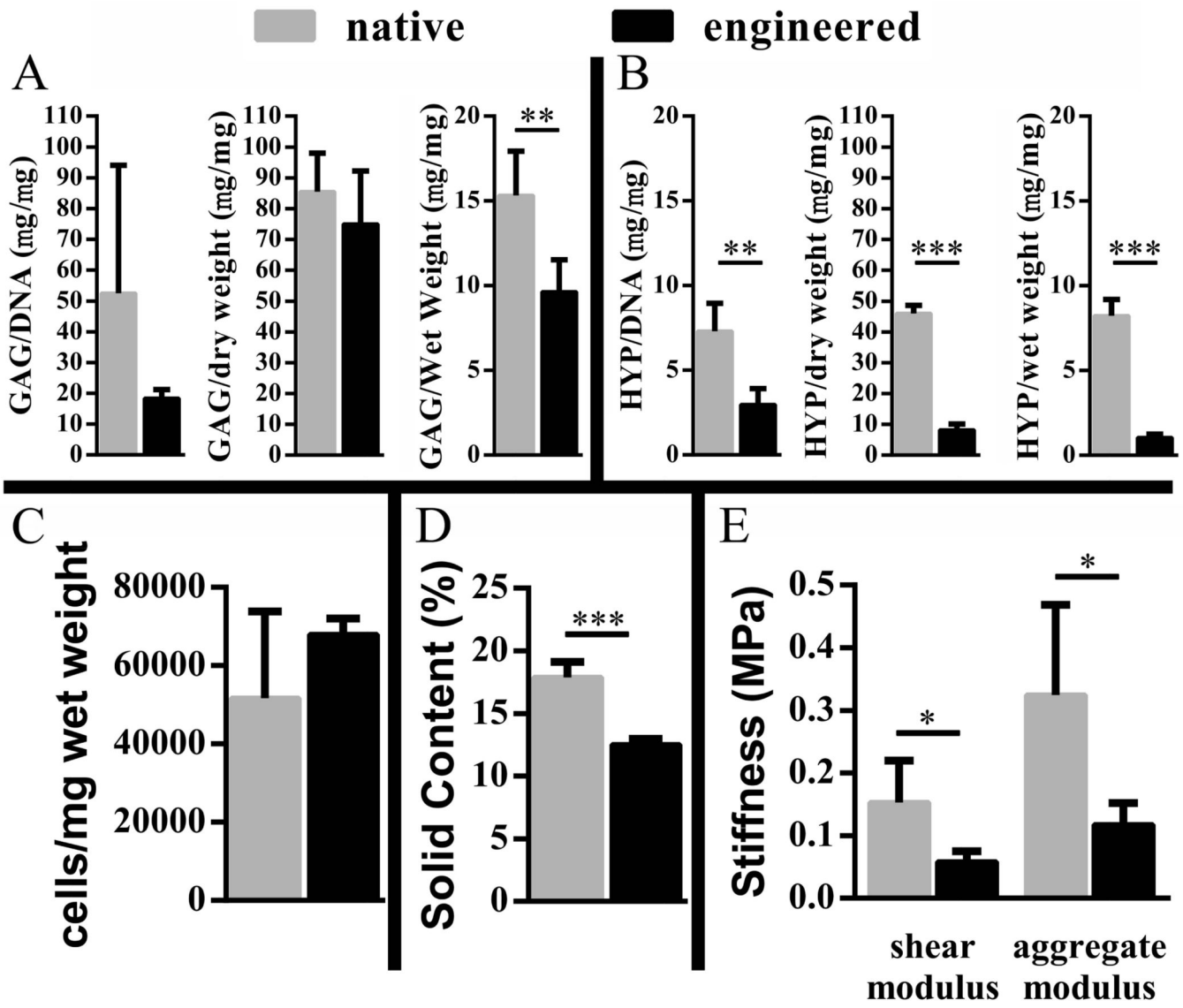

Figure 6. Composition and biomechanical properties

Comparison of ECM composition by GAG (A) and HYP (B) content, cellularity (C), solid content (D), and the stiffness (E) of engineered constructs to native cartilage. Note the change in scale in graphs of A and B; *$p < 0.05$, **$p < 0.01$, ***$p < 0.0001$.

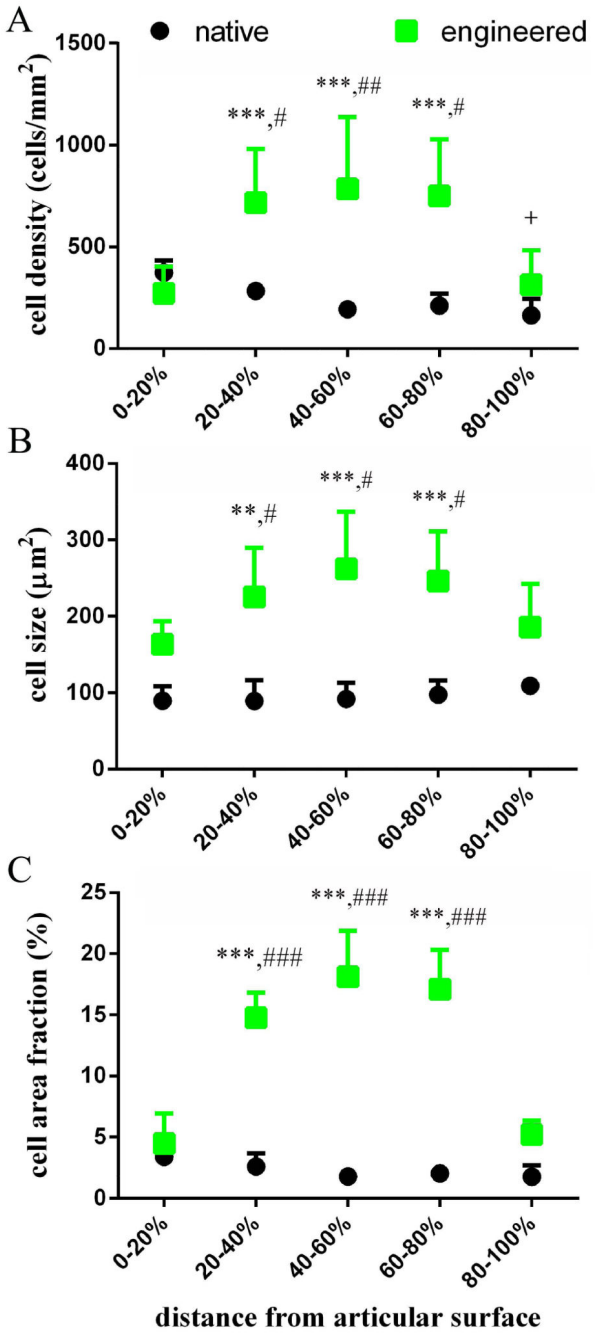

Figure 7. Depth-dependent cellularity

Patterns of cellularity varied between native cartilage and TE cartilage, and correspond to observed patterns of damage. Statistical significance was assessed within cartilage type by comparing each region to the 0-20% region (* and + for TE and native respectively), and by comparing each region between cartilage types (#). In each case, one symbol indicates $p < 0.01$, two indicates $p < 0.001$, and three indicates $p < 0.0001$.

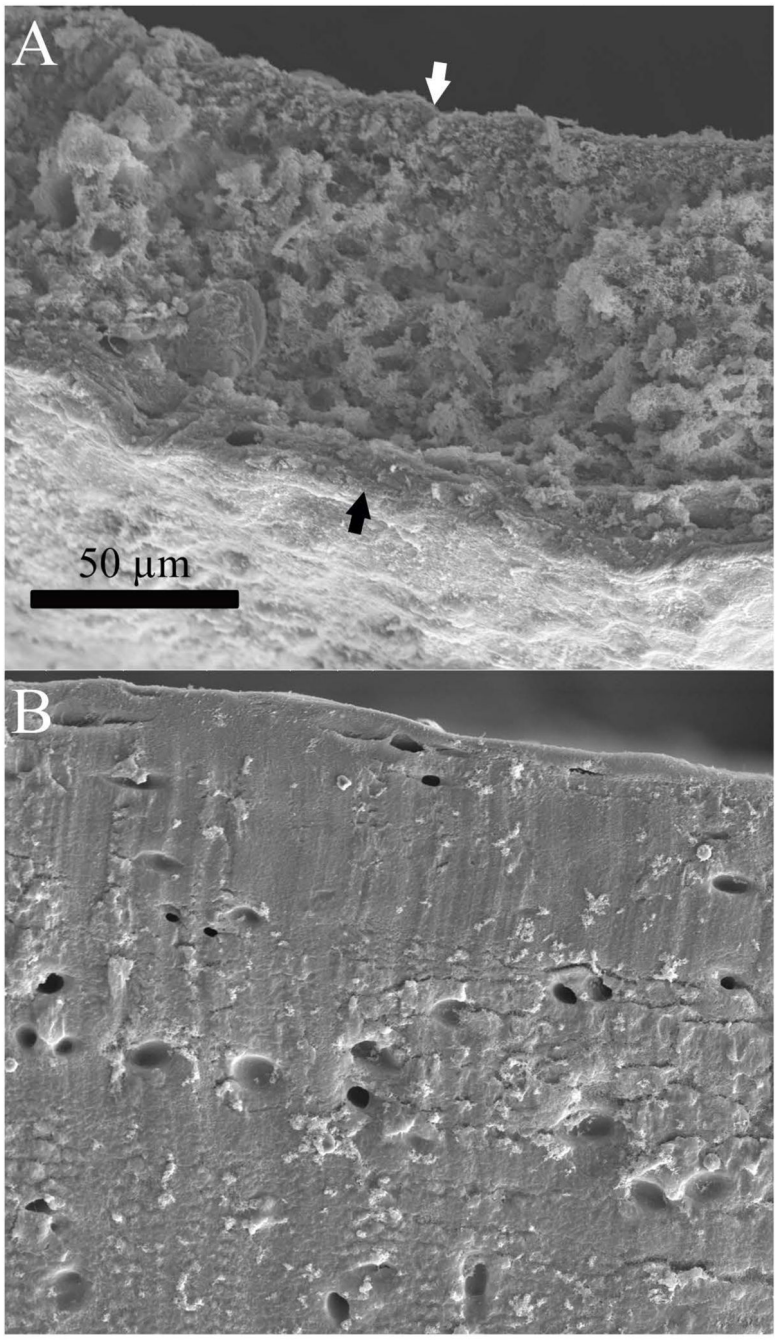

Figure 8. SEM of engineered and native cartilage

Cross sections of engineered (A) and native (B) cartilage imaged by SEM. The cross sectional face of the engineered cartilage is shown between the black and white arrows. Both images are presented at the same scale. At this magnification native cartilage appeared to be a solid material with distinct lacunae, while engineered cartilage appeared less dense, with many more lacunae.

Table 1

Frictional shear and damage experimental conditions

Experiment	Configuration	V (mm/s)	Oscillation Mode	Tissue Type		Lubricant	Normal Load	n
1	curved	25.4	intermittent	TE		PBS	0.44 N/mm	3
				native	thinned, WSZ	PBS	0.75 N/mm	3
2	curved	1	continuous	TE		PBS	0.44 N/mm	3
				native	thinned, WSZ	PBS	0.75 N/mm	4
				native	thinned, SZR	PBS	0.75 N/mm	6
3	flat	1	continuous	TE		PBS	0.55 MPa	4
				TE		PI	0.55 MPa	6
				native	full thickness	PBS	0.55 MPa	6
				native	full thickness	PI	0.55 MPa	6
4	flat	1	continuous	TE		PBS, PI	0.55 MPa	10
				native	full thickness	PBS, PI	0.55 MPa	8
5	flat	1	continuous	TE		PBS	0.55 MPa	7
				TE fresh	full thickness	PBS	0.55 MPa	8
6	flat, no adhesive	1	continuous	TE		PBS	0.55 MPa	6
				native	full thickness	PBS	0.55 MPa	6

TE = tissue engineered with freeze/thaw, WSZ = with superficial zone, SZR = superficial zone removed, PBS=phosphate buffered saline, PI = protease inhibitor